

ON THE EFFECTS OF SUPPORTING FIBERS AND NATURAL CONVECTION ON FUEL DROPLET VAPORIZATION

Frédéric RENAUD*, Christian CHAUVEAU, Iskender GÖKALP

*e-mail : frenaud@cns-orleans.fr

Laboratoire de Combustion et Systèmes Réactifs
Centre National de la Recherche Scientifique
1C, avenue de la Recherche Scientifique
45071 Orléans Cedex 2

ABSTRACT

Experimental studies on the vaporization of n-decane droplets in nitrogen are reported. To investigate the effects of the supporting fiber, two different techniques were employed, the "suspending fiber" and the new "cross fiber" technique using thin quartz wires. In addition to the heat flux provided at the droplet surface, the supporting fiber creates a conductive heat flux toward the droplet interior that rises the liquid-phase temperature. This additional heat flux is proportional to the cross section of the fiber. Therefore, the cross fiber technique is shown to cause very little perturbation to the vaporization process.

Experiments were also conducted under microgravity conditions from 567 to 967 K. At the lowest range of ambient temperatures, the regression of the droplet square diameter is not linear with time as observed in normal gravity but gradually slows down. This behavior is attributed to gas-phase unsteadiness. In microgravity, as natural convection is negligible, the fuel vapor is dispersed in the environment by mass diffusion only, which occurs at a slower rate. Fuel vapor remains around the droplet, so that the concentration gradient decreases and the phase-change mechanism is affected. For higher ambient temperatures, mass diffusion is enhanced and the linear evolution is reached.

INTRODUCTION

In many energetic systems such as diesel and rocket engines, the fuel is supplied as a spray of droplets inside the combustion chamber. It has been established that in most cases, as the spray ignites, the droplets at the center are affected by the flame as a heat source and undergo pure vaporization without burning individually. In the spray, vaporizing droplets strongly influence one another because they locally modify the temperature and fuel vapor concentration of the surrounding gas. However, the isolated droplet configuration has been intensively investigated as it allows a detailed description of the heat and mass transfers occurring during vaporization without considering complex interaction effects.

The Quasi-steady theory (QS), formulated by Godsave [1] and Spalding [2], was developed in the early 1950s for isolated droplet vaporization and combustion. This theoretical model is based on several simplifying assumptions, detailed by Law [3], such as both gas and liquid phases steady behavior and constant thermodynamic and transport properties, leading to an analytic resolution of the conservation equations. The QS theory predicts a linear evolution of the droplet surface area with time and provides an estimate of the vaporization rate :

$$K = 8 \frac{\lambda_g}{\rho_l C_{pg}} \ln(1 - Y_{fs}) \quad (1)$$

Although this theory is widely used in spray calculations because of its simplicity, some important aspects of the droplet vaporization phenomenon are not taken into account. In particular, the existence of a transient heat-up period was evoked [4, 5]. During the initial stage of the droplet lifetime, vaporization does not occur or is eventually very slow as the heat flux provided by the environment is required to rise the temperature of the droplet surface. Moreover, in most experimental configurations, the droplet is maintained by a material support, generally a thin quartz or glass fiber. It has been mentioned [3] that the fiber influences vaporization as it creates an additional heat transfer by conduction inside the liquid-phase. This disagrees with the theoretical model and needs to be considered. The effect of the fiber on the vaporization rate was studied experimentally [6, 7] and numerically [7].

The gas-phase steady behavior has been discussed and analyzed from an analytical and numerical point of view. In the model of Crespo and Linan [8] which includes time-depending terms, unsteady effects are due to the inertia of the liquid-phase relative to the surrounding gas. Unsteady droplet vaporization models were later extended to high ambient conditions [9, 10]. Also, one of the most stringent assumptions made in numerical simulations is the spherical symmetry of the droplet and the temperature and fuel vapor concentration profiles of the surrounding gas. In practical situations, this assumption is not valid because of natural and forced convection. For this reason, microgravity conditions are required to eliminate all convection effects and to approach conditions similar to the theoretical ones.

The aim of this paper is to study the effect of the supporting material by employing two different techniques. We compare the experimental results to the QS theory and focus on the conductive heat transfer through the fiber that enhances vaporization. We also present the results obtained under microgravity conditions. We observe that, due to gas-phase unsteadiness, the vaporization mechanism is different from that under normal gravity.

EXPERIMENTAL

The experimental set-up is schematically represented on Fig. 1. The furnace, generating high temperatures up to 1200 K by Joule effect, is placed into the pressure chamber. The inner dimensions of the furnace are 68 mm diameter and 100 mm height, which provides an inner volume of 0.36 L. The experiments were performed using two different techniques to support the droplet (see Fig. 2), in order to emphasize the effects of the supporting material on the vaporization process. The first technique is the commonly employed "suspending fiber", which consists of a quartz fiber with a thickened spherical tip. The second one was developed by taking into account the disturbances caused by the suspending fiber technique, as discussed in the introduction. It is called the "cross fiber" technique ; the droplet is created at the intersection of two 14 μm diameter quartz wires fixed perpendicularly on a frame. In both cases, a piezo-electric injector generates the droplet, by supplying a liquid jet impacting the support.

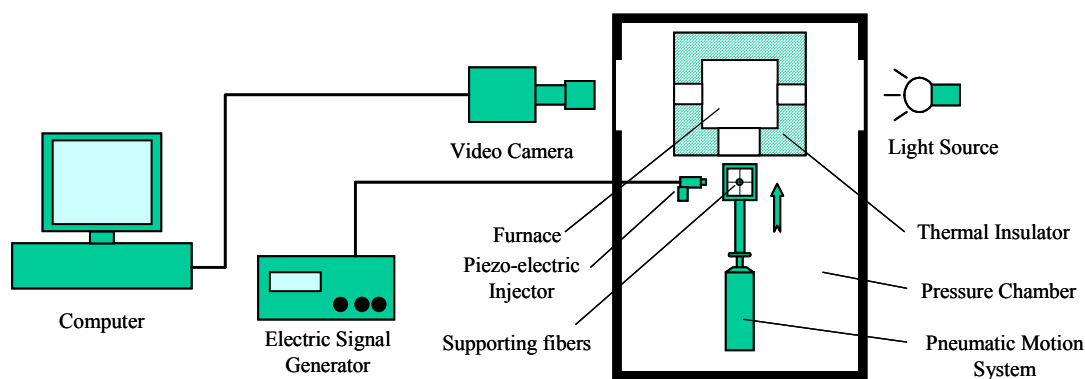


Figure 1 : Schematic representation of the experimental set-up.



Figure 2 : Droplet supporting technique. (a) Suspending fiber, (b) Cross fiber.

N-decane $\text{C}_{10}\text{H}_{22}$ was selected as the liquid fuel, vaporizing in a Nitrogen gaseous environment. The droplet is initially in the lower part of the chamber. A pneumatic motion system allows the droplet to be introduced into the furnace where vaporization occurs. The vaporizing droplet is recorded by a high-speed video camera with a frame rate of 150 to 750 frames/s. Each vaporization sequence contains about 700 images to obtain a satisfactory temporal resolution. The images are transferred to a computer and analysed with a binarisation method. The mean uncertainty on the determination of the droplet diameter is of the order of 3%. In addition, a given experiment is performed at least 3 times to check the repeatability of the data. For instance, the vaporization rate at $T_\infty = 767 \text{ K}$ lies between $0.183 \text{ mm}^2/\text{s}$ and $0.190 \text{ mm}^2/\text{s}$, which provides $\pm 2\%$ uncertainty. The structure of the set-up was designed to be integrated inside the A300 Aircraft of CNES for parabolic flights, to achieve microgravity conditions of $10^{-2}g_0$ for 22 s duration.

RESULTS AND DISCUSSION

Effect of the droplet supporting technique

The experiments were conducted for ambient temperatures varying from 567 K to 967 K, at normal pressure in normal gravity. The supporting technique selected was the cross fiber technique, using 14 μm diameter quartz wires.

With this technique, the droplet shape can be reasonably assumed as spherical (see Fig. 2b). The initial droplet diameter d_0 was of the order of 500 μm . The evolution of $(d/d_0)^2$ is plotted against t/d_0^2 for various ambient temperatures on Fig. 3. As these evolutions are considered to be linear, we define the vaporization rate as the slope of each curve. On Fig. 4, the vaporization rate is represented as a function of temperature. We also indicate the QS values, calculated by Eq. (1) according to the method of Lefebvre [11]. At the lowest temperature, the experimental vaporization rate is approximately half the theoretical one, and remains lower over the range of temperatures investigated.

This poor agreement is due to the fact that, to obtain the QS vaporization rate, a significant assumption is made that all the energy supplied by the ambient gas is used for the phase-change mechanism :

$$\frac{1-Y_{fs}}{Y_{fs}} C_{pg}(T_{\infty} - T_s) = L_v \quad (2)$$

This assumption implies that, since no energy is required to heat-up the droplet interior, its temperature is uniform and constant, equal to the wet-bulb temperature, through the vaporization period. In the experiments, the droplet is initially at room temperature. A part of the heat flux reaching the droplet is necessary to heat-up the liquid phase, so that the droplet surface temperature rises to reach a value that allows for vaporization. The first consequence is that the center of the droplet is always colder than its surface, as observed numerically [9]. However, the linear shape of the vaporization curves indicates that an equilibrium state is attained at the droplet surface between the gas and liquid heat fluxes and the latent heat of vaporization all along the droplet lifetime. The second consequence is that less energy is available for the effective vaporization, which finally results in an experimental vaporization rate lower than the theoretical value.

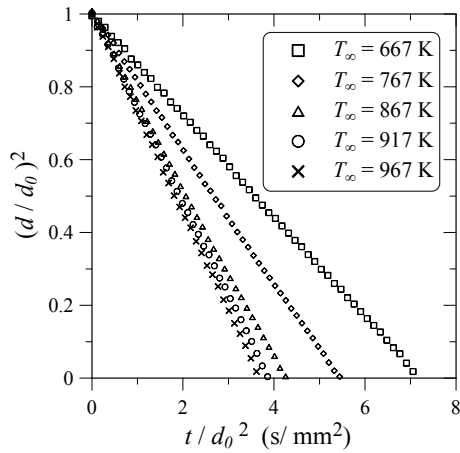


Figure 3 : Vaporization curves using the cross fiber technique.

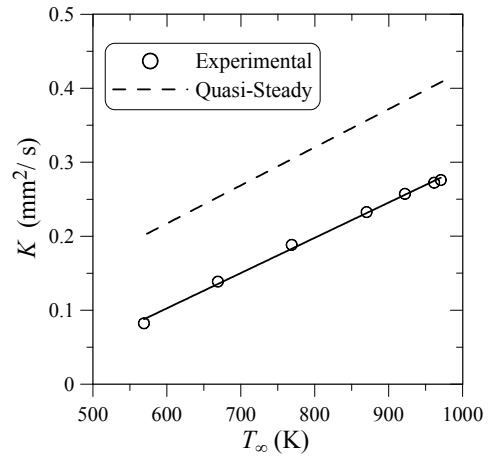


Figure 4 : Experimental and theoretical evolution of the vaporization rate with ambient temperature.

Moreover, in the experiments, the droplet is supported by quartz fibers. To investigate the influence of the supporting material on the vaporization mechanism, we conducted further experiments at a fixed ambient temperature, $T_{\infty} = 570$ K, using both the cross fiber technique with 14 μm diameter wires and the suspending fiber technique with 3 different fiber diameter values, $d_f = 106$ μm , $d_f = 144$ μm and $d_f = 181$ μm . The initial droplet diameter was kept constant in all cases at $d_0 = 800$ μm to prevent the differences to be attributed to buoyancy effects. The corresponding vaporization curves are plotted on Fig. 5. As the droplets are bigger than in our previous experiments, the initial heat-up period mentioned in the introduction appears. We also observe enhanced droplet diameter regression rates in the latter part of the curve, in the case of the suspending fiber. Consequently, the vaporization rate is defined on the linear part of each curve. The value of the vaporization rate obtained at this ambient temperature with the cross fibers is slightly higher than previously because of buoyancy effects due to the larger value of d_0 .

Although quartz is supposed to have a very low thermal conductivity ($\lambda_f = 1.38$ W/m K), a conductive heat transfer exists from the fibers toward the interior of the liquid-phase which adds to the heat transfer at the droplet surface. This additional heat flux reduces the energy used to increase the liquid temperature required at the droplet surface. The higher this heat flux is, the higher the energy remaining for vaporization, and thus the higher the vaporization rate for the same ambient temperature. A relevant aspect of the effect of the fiber is the enhanced vaporization rate in the latter part of the droplet lifetime. As the volume of the droplet becomes comparable with the volume of the fiber, the net liquid volume vanishes and gets easier to heat-up.

On Fig. 6, the vaporization rate is plotted as a function of the square diameter of the quartz fiber, d_f^2 . This evolution is observed to be linear, that can be justified as follows. Due to the low diameter of the fiber, the conductive heat flux propagating through it can be considered as monodimensional. This means that the heat flux is proportional to the cross section of the fiber, or equivalently to d_f^2 . On an other hand, the vaporization rate K , referring to Fig. 4, depends linearly on ambient temperature T_{∞} , both experimentally and theoretically. Since the heat flux, within the context of the QS

theory, is proportionnal to $(T_\infty - T_s)$ and the surface temperature T_s is approximately constant, the vaporization rate also evolves in a linear way with the heat flux. We consider a given value of the vaporization rate, called K_0 , corresponding to the case in which all the heat is provided to the droplet through its surface, namely no fiber effect occurs. We find that the difference between the actual vaporization rate K and the "ideal" one K_0 is proportional to the heat flux through the fiber, and equivalently to d_f^2 .

The extrapolation of the linear function passing by the experimental points to $d_f^2 = 0$ provides the value of K_0 , free from the fiber effect. This value is very close to that obtained with the cross fiber technique, which means that our experimental configuration causes no disturbance in the vaporization process. In a similar way, the intersection of the linear fit with the QS value indicates the value of the fiber diameter $d_f(QS) \approx 320 \mu\text{m}$ (which does not appear on the graph). This value is such that all the heat flux necessary to rise the temperature of the droplet comes from the fiber, therefore all the energy required for vaporization is provided at the droplet surface, following the QS assumption.

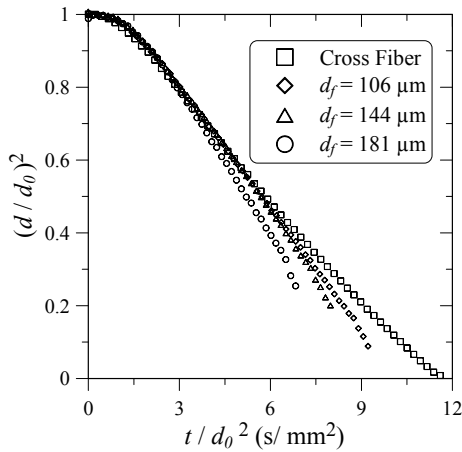


Figure 5 : Vaporization curves for various fiber diameters at $T_\infty = 570 \text{ K}$.

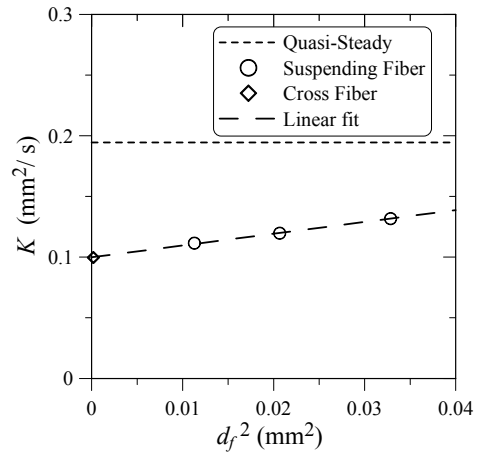


Figure 6 : Evolution of the vaporization rate with the square diameter of the fiber.

Effect of the gravity conditions

Experiments in microgravity were conducted at a fixed ambient temperature, $T_\infty = 567 \text{ K}$, and at normal pressure. By using the cross fiber technique, the initial diameter of the droplet varied from 0.2 mm to 0.5 mm. The time evolution of the square diameter of the droplet for several initial diameter values is represented on Fig. 7. The vaporization curves, except for the smallest droplet, are not linear contrary to the observation in normal gravity. We can define a transition time of about 1.5 s, during which the vaporization rate gradually decreases. After this transition time, the vaporization curves remain approximately linear. In the case of the smallest droplet, the vaporization curve is considered as linear.

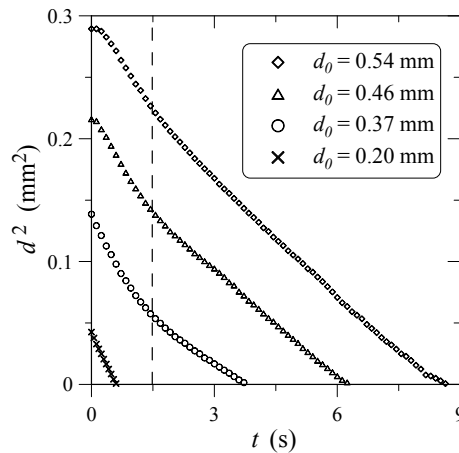


Figure 7 : Vaporization curves for several initial diameter values at $T_\infty = 567 \text{ K}$.

The following interpretation for the appearance of the transition time is proposed. In the vaporization process, the role of natural convection in normal gravity is to disperse the fuel vapor in the environment, to maintain a constant concentration gradient at the surface of the droplet. Under microgravity, natural convection is suppressed and mass

diffusion is the dominant transport process, which slows down with increasing the diffusive surface area. At the initial stage of vaporization, the fuel vapor, which is at its saturation value at the droplet surface, is transported in the fuel vapor free environment. Due to the diffusion process, a distance far enough from the droplet exists at which the vapor diffusion velocity becomes negligible. This implies that, when vaporization progresses, the thickness of the fuel vapor layer enlarges and the concentration gradient decreases. The phase-change mechanism adapts until the fuel vapor production balances its evacuation toward infinity. Once the "diffusive concentration profile" has been established, a linear evolution can be achieved.

Referring to Fig. 7, the transition time does not depend on the initial size of the droplet ; this characterizes the diffusive transport process within the gas-phase. Considering that the diffusion velocity at the surface of a large droplet is lower than that of a smaller one, the thickness of the concentration profile, comparatively to its diameter, is smaller. In addition, for the same variation of the surface area, the production of fuel vapor is higher in the case of the large droplet. For these reasons, the time required to establish the concentration profile is shorter, comparatively to the total vaporization time, for a large droplet. Similarly, in our experiments, the vaporization time of the smallest droplet is shorter than the transition time. The fuel vapor is never accumulated in a bounded region and the phase-change mechanism is not affected, which leads to a linear evolution.

As mentioned in numerical studies [8, 10], the transition time, due to gas-phase unsteadiness, can be related to the density ratio ρ_∞/ρ_l . This ratio represents the inertia of the liquid-phase in comparison with that of the surrounding gas, depending on the ambient conditions. Experiments were performed for ambient temperatures varying from 667 K to 967 K, for a fixed value of the initial droplet diameter, $d_0 = 0.37$ mm. The vaporization curves are plotted on Fig. 8. In order to quantify the non-linear shape of the vaporization curves, we define the "deviation factor" as :

$$\Delta = (1 - t/t_v) - (d/d_0)^2 \quad (3)$$

where t_v is the total vaporization time. Its evolution, referring to the corresponding vaporization curves, is represented on Fig. 9. With reducing the gas density by increasing ambient temperature, the density ratio decreases and unsteady effects are supposed to disappear. The deviation is stronger at $T_\infty = 667$ K and reduces as temperature rises, indicating that the vaporization curves become more and more linear. We can assume that, at a sufficiently high temperature, the distance of negligible diffusion velocity mentioned previously increases to approach infinity. From the point of view of the fuel vapor evacuation, this situation is qualitatively equivalent to that of a very small droplet at a lower temperature.

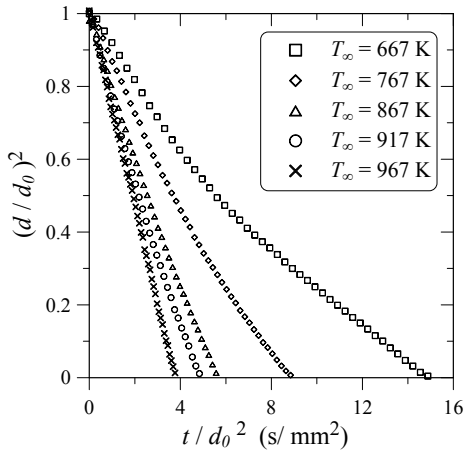


Figure 8 : Vaporization curves for various ambient temperatures with $d_0 = 0.37$ mm.

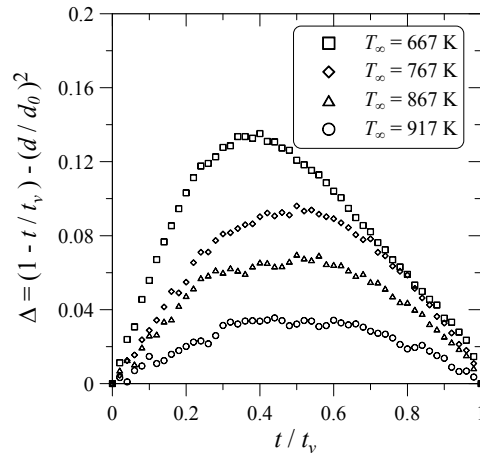


Figure 9 : Deviation from linearity of the vaporization curves as a function of normalized time.

CONCLUSION

In normal gravity, the experimental vaporization rate obtained by using the cross fiber technique with $14 \mu\text{m}$ diameter quartz wires is significantly lower than the QS value over the range of temperatures investigated, although the temporal evolution of the droplet square diameter is linear in both cases. In the experiments, a part of the heat flux provided to the droplet is needed to heat-up the liquid-phase through the total vaporization time, reducing the heat flux used for effective vaporization. Moreover, an additional heat flux by conduction exists through the supporting fiber and varies linearly with the square diameter of the fiber. By extrapolation to zero fiber diameter, we obtain a value of the vaporization rate such that no heat transfer through the fiber occurs ; this value is very close to that obtained with our cross fiber technique.

Experiments in microgravity show the appearance of a transition time during which the vaporization curves are not linear. As mass diffusion is the only transport process in this situation, at a given distance from the droplet the fuel vapor diffusion velocity becomes negligible, implying that the fuel vapor layer enlarges and the concentration gradient decreases. After the transition time, the diffusive concentration profile is established and the production of fuel vapor at

the droplet surface balances its evacuation in the environment. With increasing ambient temperature, the shape of the vaporization curves is more and more linear. At a sufficiently high temperature, the distance of negligible diffusion velocity approaches infinity, in comparison to the size of the droplet. The fuel vapor can be evacuated instead of remaining in a bounded region, so that the phase-change mechanism is not affected through the entire droplet lifetime.

ACKNOWLEDGMENTS

This work is supported by the CNRS, the CNES and the Region Centre. FR is supported by a joint grant from the CNES and the Region Centre.

NOMENCLATURE

$C_{p g}$	Specific heat at constant pressure of the gaseous mixture	J/kg K
d	Diameter of the droplet	m
d_0	Initial diameter of the droplet	m
d_f	Diameter of the quartz fiber	m
g_0	Gravity acceleration	m/s ²
K	Vaporization rate	m ² /s
K_0	Vaporization rate with no fiber effect	m ² /s
L_v	Latent heat of vaporization	J/kg
t	Time	s
t_v	Total vaporization time	s
T_s	Temperature of the droplet surface	K
T_∞	Ambient temperature	K
Y_{fs}	Mass fraction of the fuel at the droplet surface	dimensionless
Greek symbols		
Δ	Deviation factor	dimensionless
λ_g	Thermal conductivity of the gaseous mixture	W/m K
λ_f	Thermal conductivity of the quartz fiber	W/m K
ρ_∞	Density of the ambient gas	kg/m ³
ρ_l	Density of the droplet	kg/m ³

REFERENCES

1. G.A.E. Godsave, Studies of the combustion of drops in a fuel spray – The burning of single drops on fuel, *Fourth Symposium (International) on combustion*, The Combustion Institute, pp. 818-830, 1953.
2. D.B. Spalding, The combustion of liquid fuels, *Fourth Symposium (International) on combustion*, The Combustion Institute, pp. 847-864, 1953.
3. C.K. Law, Recent advances in droplet vaporization and combustion, *Prog. Energy Combust. Sci.*, Vol. 8, pp. 171-201, 1982.
4. J.S. Chin and A.H. Lefebvre, The role of the heat-up period in fuel dropl evaporation, *Int. J. Turbo Jet Engines*, Vol.2, pp. 315-325, 1985.
5. H. Nomura, Y. Ujiie, H.J. Rath, J. Sato and M. Kono, Experimental study on high-pressure droplet evaporation using microgravity conditions, *Twenty-Sixth Symposium (International) on combustion*, The Combustion institute, pp. 1267-1273, 1996.
6. G.R. Toker and J. Stricker, Holographic study of suspended vaporizing volatile liquid droplets in still air, *Int. J. Heat Mass Transfer*, Vol. 39, pp. 3475-3482, 1996.
7. J.R. Yang and S.C. Wong, An experimental and theoretical study of the effects of heat conduction through the support fiber on the evaporation of a droplet in a weakly convective flow, *Int. J. Heat Mass Transfer*, Vol. 45, pp. 4589-4598, 2002.
8. A. Crespo and A. Linan, Unsteady effects in droplet evaporation and combustion, *Combust. Sci. Technol.*, Vol. 11, pp. 9-18, 1975.
9. H. Jia and G. Gogos, High pressure droplet vaporization ; effects of liquid-phase gas solubility, *Int. J. Heat Mass Transfer*, Vol. 36, pp. 4419-4431, 1993.
10. M. Arias-Zugasti, P.L. Garcia-Ybarra and J.L. Castillo, Unsteady effects in droplet vaporization lifetime at subcritical and supercritical conditions, *Combust. Sci. Technol.*, Vol. 153, pp. 179-191, 2000.
11. A.H. Lefebvre, Drop evaporation, in N. Chigier (ed.), *Atomization and Sprays*, chap. 8, Hemisphere Publishing Corporation, New York, 1989.